

Stereo vision— Facing the challenges and seeing the opportunities for ADAS applications



Aish Dubey
ADAS

Texas Instruments

Introduction

Cameras are the most precise mechanisms used to capture accurate data at high resolution. Like human eyes, cameras capture the resolution, minutiae and vividness of a scene with such beautiful detail that no other sensors such as radar, ultrasonic and lasers can match. The prehistoric paintings discovered and dated back tens of thousands of years ago in caves across the world are testaments that pictures and paintings coupled with visual sense have been the preferred method to convey accurate information [1].

The next engineering frontier, that some might argue will be the most challenging for the technology community, is real-time machine vision and intelligence. The applications include, but are not limited to, real-time medical analytics (surgical robots), industrial machines and cars that are driven with autonomous intelligence. In this particular paper, we will focus on autonomous Advanced Driver Assistance Systems (ADAS) applications and how cameras and stereo vision in particular is the keystone for safe, autonomous cars that can “see and drive” themselves.

The key applications that require cameras for ADAS are shown below in Figure 1. Some of the applications shown can be implemented using just a vision system such as forward-, rear- and side-mounted cameras for pedestrian detection, traffic sign recognition, blind spots and lane detect systems. Others such as intelligent adaptive cruise control can be implemented robustly as a fusion of radar data with the camera sensors, especially for complex scenarios such as city traffic, curvy non-straight roads or higher speeds.

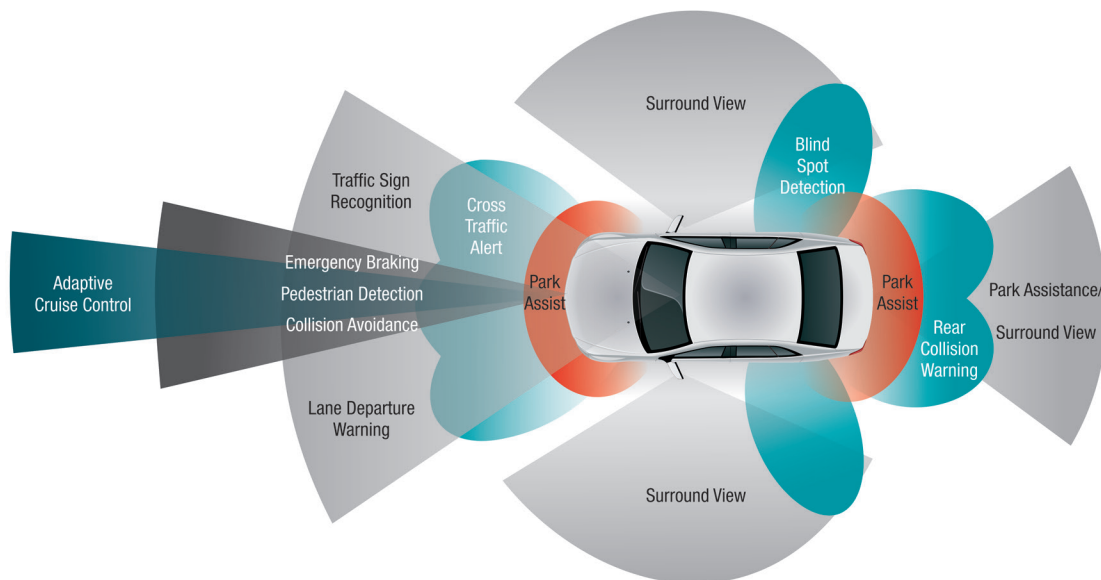


Figure 1: Applications of camera sensors for ADAS in a modern vehicle: (a) Forward facing camera for – lane detect, pedestrian detect, traffic sign recognition and emergency braking. (b) Side- and rear-facing cameras for parking assistance, blind spot detection and cross traffic alerts

What kind of camera is needed?

All the real world scenes that a camera encounters are three dimensional. The objects that are at different depths in real world may appear to be adjacent to each other in the two-dimensional mapped world of the camera sensor. Figure 2 shows a picture from the Middlebury image dataset [2]. Clearly the motor bike in the foreground of the picture is about two meters closer to the camera than the storage shelf in the background. Please pay attention to point 1 and 2 annotated in the figure. The red box (point 1) that is in the background appears adjacent to the forks (2) of the bike in the captured image, even though it is at least two meters farther away from the camera. Human brain has the power of perspective that allows us to make the decision about depth from a 2-D scene. For a forward-mounted camera in the car, the ability to analyze perspective does not come as easy.

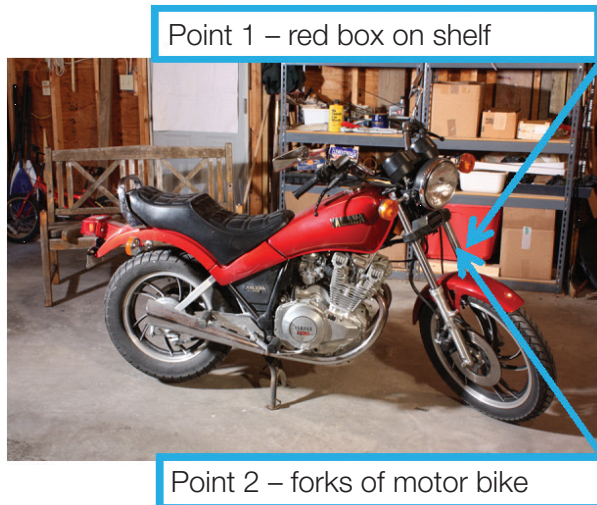


Figure 2: Image from 2014 Middlebury database. The motor bike in the foreground is much closer to the camera than the storage shelf, though all objects appear adjacent in a 2-D mapped view.

If we have a single camera sensor mounted and capturing video that needs to be processed and analyzed, that system is called a monocular (single-eyed) system, whereas a system with two cameras, separated from each other is called a stereo vision system. Before we go any further, please have a look at Table 1 that compares the basic attributes of a monocular-camera ADAS with a stereo-camera system.

Comparison parameter	Mono-camera system	Stereo-camera system
Number of image sensors, lenses and assembly	1	2
Physical size of the system	Small (6" × 4" × 1")	Two small assemblies separated by ~25–30 cm distance
Frame rate	30 to 60 frames per second	30 frames per second
Image processing requirements	Medium	High
Reliability of detecting obstacles and emergency braking decisions	Medium	High
System is reliable for	Object detection (lanes, pedestrians, traffic signs)	Object detection "AND" calculate distance-to-object
System cost	1×	1.5×
Software and algorithm complexity	High	Medium

Table 1: High-level comparison of system attributes for a mono- vs. stereo-camera ADAS system

The monocular-camera-based video system can do many things reasonably well. The system and analytics behind it can identify lanes, pedestrians, many traffic signs and other vehicles in the path of the car with good accuracy. Where the monocular system is not as robust and reliable is in calculating the 3-D view of the world from the planar 2-D frame that it receives from the single camera sensor. That's not surprising if we consider the natural fact that humans (and most advanced) animals are born with

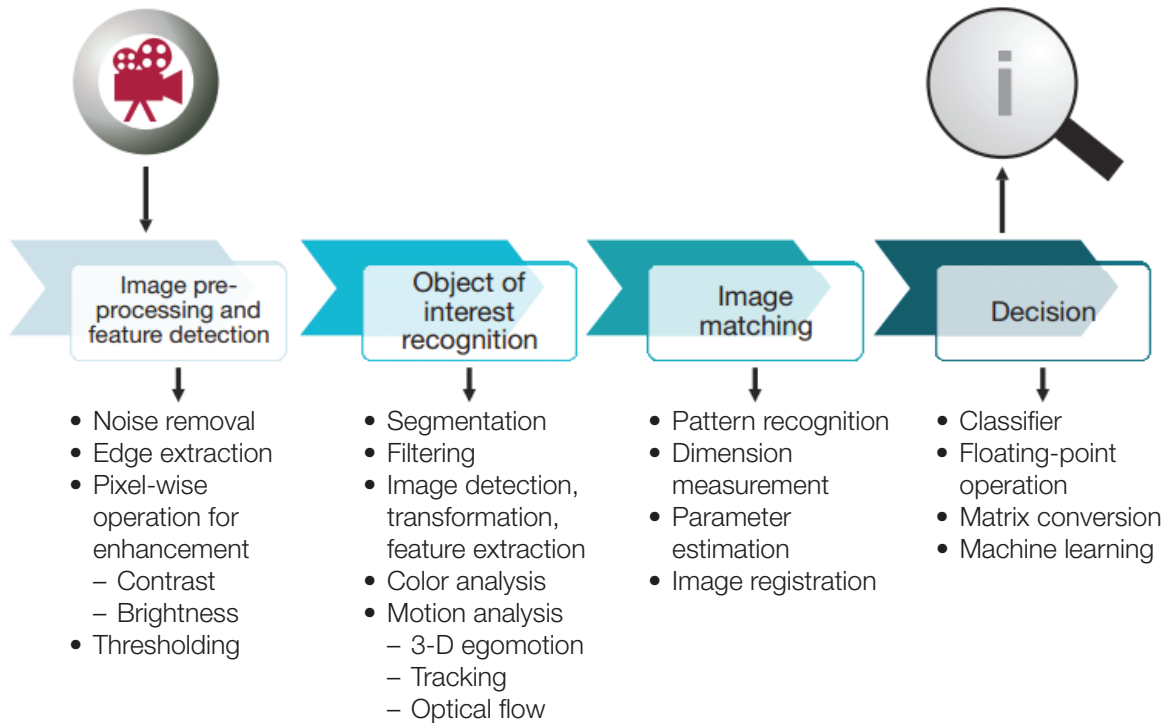


Figure 3: High-level algorithm flow and processes for analyzing an image in ADAS system

two eyes. Before analyzing this problem in further detail, please take a look at Figure 3. This figure describes at high level the process and algorithms used to analyze the video (image) frame received from a camera sensor.

The first stage in Figure 3 is the image pre-processing step, where various filters are run on the image (typically every pixel), to remove sensor noise and other un-needed information. This stage also converts the format of the received BAYER data from camera sensor to a YUV or RGB mode that can be analyzed by subsequent steps. On the basis of the preliminary feature extraction (edges, haar, Gabor filters, Histogram of oriented gradients, etc.) done in this first stage, the second and third stages further analyze the images to identify regions of interest by running algorithms such as segmentation, optical flow, block matching and pattern recognition. The final stage utilizes region information and feature data

generated from the prior stages to create intelligent analysis decisions about the class of the object in the regions of interest. This brief explanation does not quite do justice to the involved ADAS image-processing algorithms' field, however since the primary objective of this article is to highlight the additional challenges and robustness that a stereo vision system provides, the block-level algorithmic information is sufficient background for us to delve deeper into the topic.

How does a monocular camera measure distance to an object from 2-D data?

There are two distinct possibilities through which the distance measurement is performed by a monocular camera. The first of these is based on the simple

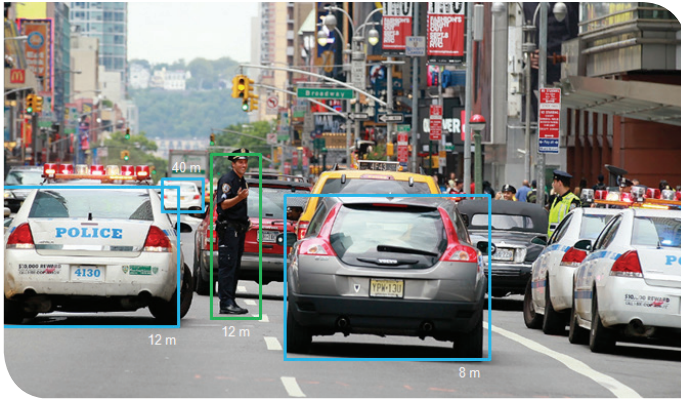


Figure 4: A picture showing various identified objects and their estimated distance from a monocular camera. It is clear that the more the distance of the identified object from the car, smaller is the maximum covering rectangle size ^{[3], [17]}.

premise that the objects closer to the camera appears bigger, and therefore takes up a larger pixel area in the frame. If an object is identified as a car, then the size of the object can be approximated by a maximum-covering-rectangle drawn around it. The bigger the size of this rectangle, the closer that object is to the camera (i.e. the car). The emergency braking algorithm will assess if the distance to each object identified in the frame is closer than a safe predefined value, then initiate the collision avoidance or driver warning actions as necessary. See Figure 4 for a simple illustration of this idea.

Simplicity and elegance are both benefits of this method, however there are some drawbacks to this approach. The distance to any identified object cannot be assessed until the object is pre-identified “correctly”. Consider the scenario shown in Figure 5. There are three graphical pedestrians shown in this figure. Pedestrian 1 is a tall person, while pedestrian 2 is a shorter boy. The distance of both these individuals to the camera is same. The third pedestrian (3) shown in the picture is farther away from the camera, and is again a tall person. Here the object detection algorithm will identify and draw rectangles around the three identified pedestrians.

Unfortunately the size of the rectangle drawn around the short boy (individual 2), who is much closer to the camera than the tall person (individual 3) who is farther will be equal. Therefore, size of an identified object in pixels on the captured 2-D frame is not a perfectly reliable indicator of the distance of that object from the camera. The other issue to consider is if an object remains unidentified in a scene, then its distance cannot be ascertained, since the algorithm does not know the size of the object (in pixels). The object can remain unidentified for a multitude of reasons such as occlusion, lighting and other image artifacts.

The second method which can be utilized to calculate the distance of an object using monocular cameras is called “structure-from-motion (SFM)”. Since the camera is moving hence in theory, consecutive frames captured in time can be

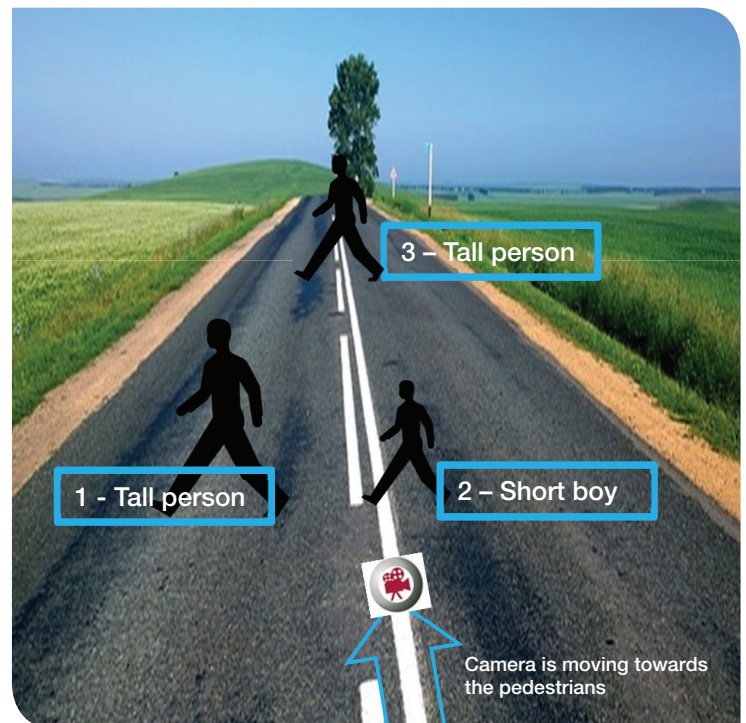


Figure 5: A virtual info-graphic showing 3 pedestrians in the path of a moving vehicle with camera. The pixel size of the individuals 3 and 2 are exactly same, however individual 2 is much closer to the vehicle than individual 3. ^[4]

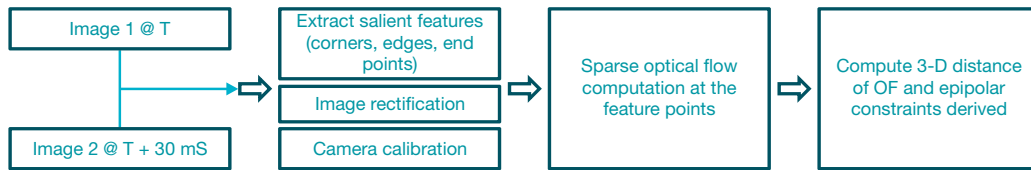


Figure 6: A high-level data flow for SFM-based distance calculation. The sparse optical flow (OF) may be replaced with the dense flow calculation (for every pixel) as well. The above flow assumes 30 fps.

compared against each other for key features. Epipolar geometry defines constrained parameters for where a given point in 3-D space can move to in two consecutive frames captured by a moving (translated and possibly rotated) camera. SFM is an involved topic by itself and therefore in this article, we will draw attention to the challenges of distance computation using SFM rather than the mechanics and mathematics of how it is done. For readers who are deeply interested in how SFM works Reference [5] is a good summary. It is sufficient here to understand a high-level flow of how an SFM algorithm works (Figure 6).

Given the data flow, it is easy to understand the challenges the SFM-based distance computation

Parameter	Challenges of SFM-based distance computation
Images not captured simultaneously	Unlike stereo, the camera does not capture two frames simultaneously. SFM operates on temporal frames. Therefore, the movement of the camera needs to be captured “accurately”. In an automotive scenario, that information is based on the accurate data of vehicle speed, steering angles, etc. An online and continuous camera rig calibration is not as accurate as a fixed, pre-calibrated stereo camera rig. Because of temporal discontinuity, critical intensity differences may appear in the image. Occlusions appearing in the image due to temporal discontinuity make feature correspondence difficult.
Computation requirements	A dense optical flow is computationally expensive compared to a dense stereo flow. A sparse optical flow may miss out on critical features that don’t match in two images.
Noisy images	Noise assumptions (brightness constancy) may be violated more for a temporal series of images compared to two images captured simultaneously. Need to over-constrain and over-calculate the computation to compensate for noise.

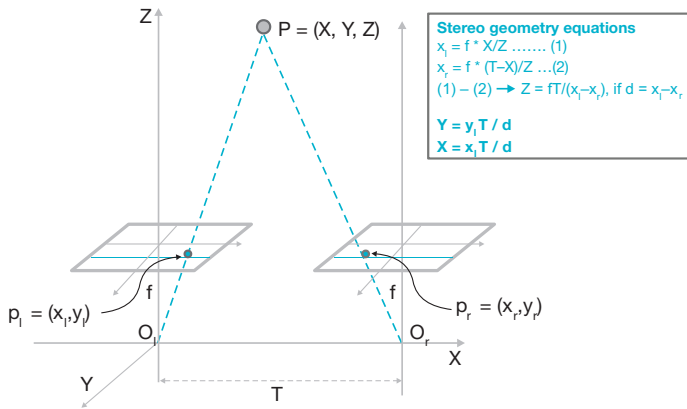
Table 2: Challenges for SFM-based distance computation

faces for a monocular camera system. Please see Table 2 for the list of these issues.

How does stereo vision calculate distance of objects from 2-D planar data?

Before radars were invented, ships already used stereo reflection mechanisms coupled with a clockwork dial to calculate distance of enemy or pirate ships. (This information would then be used to aim the cannon at enemy ships.) There were two, sometimes more, mirrors (stereo) mounted on each side of the ship hull. A system of carefully arranged reflection mirrors relayed the images from the primary stereo mirrors to a control station. An operator on the control station would adjust the clockwork mechanism to superimpose and align the two images received over each other. The reading on the pre-calibrated dial attached to the clockwork would indicate the distance of the enemy ship. The fundamental stereo algorithm has not changed for centuries now. Therefore, the methods are stable and reliable. The regularity and stability of algorithms allows the opportunity to design an optimum hardware machine to perform the stereo vision calculations.

Figure 7 on the following page shows the stereo geometry equations. If the two cameras are calibrated, then the problem of finding distance to an object can be reformulated to find the disparity



Stereo disparity calculation and accuracy of calculated distance

Figure 8 shows three different graphs to demonstrate the relationship between disparity and the distance-to-object. The first thing to notice is that the measured disparity is inversely proportional to the distance of an object. The closer an object is to the stereo cameras; more is the disparity and vice-versa. Theoretically, a point with zero disparity is infinitely away from the cameras. Concretely, the calculation shows that for the chosen physical parameters of the system (see Figure 8-a), a disparity of 1 pixel implies a distance of ~700 meters, while for a calculated disparity of 2 pixels, the estimated distance is ~350 meters. That is a really large resolution and if the disparity calculation is inaccurate by one pixel, then the estimated distance will be incorrect by a large amount (for longer distances > 100 meters). For shorter distances (lower part of the curves in Figure 8 < 50 meters), the resolution of distance calculation is much more improved. It is evident by the distance calculation points in the graphs

Figure 7: Stereo geometry equations. The depth of a point in 3-D space is inversely proportional to the disparity of that point between the left and right cameras. [6]

between the simultaneous images captured by the left and right cameras for that point. For pre-calibrated stereo cameras, the images could be rectified such that epipolar geometrical lines are simple horizontal searches (on the same row) for every point between two images. The disparity is then defined as the number of pixels a particular point has moved in the right camera image compared to the left camera image. This concept is crucial to remember, since it allows regular computation patterns that are amenable for hardware implementation. Before we delve deeper into this topic, the concept of disparity needs to be clarified further.

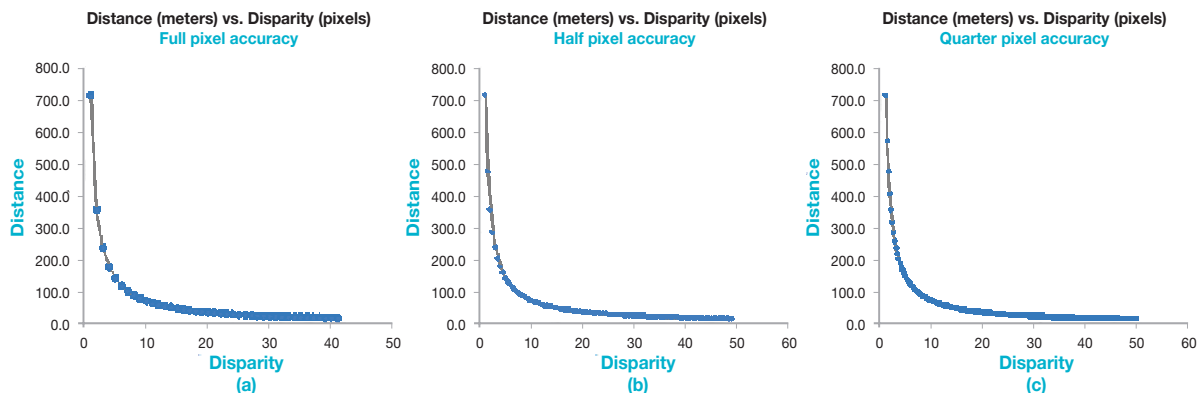


Figure 8: Distance vs. disparity graphs for different accuracy of calculation. The distance accuracy improves with increased pixelar accuracy of disparity calculation. Calculations made for (a) 30-cm distance between two cameras, (b) focal length of 10 mm, (c) pixel size of 4.2 microns.

which crowd together. In this range, if the disparity calculation is inaccurate by one pixel (or less), the calculated distance is wrong by approximately two to three meters.

There are methods to improve the accuracy of the system further. As shown by Figures 8(b) and 8(c), if the disparity calculation is performed at half or quarter pixel levels, then the resolution of distance calculation improves proportionally. In those scenarios, for distances larger than 100 meters (but less than 300 meters), the resolution of calculated distance for consecutive disparity increase is ~30–40 meters. For distances smaller than 100 meters, the accuracy can be better than 50 cms. It may be important to reiterate that the accuracy needs to be maximized (preferable to < 0.1 meters range) for a collision avoidance system operating for close distances. At the same time, operating range of the stereo camera needs to be improved, even at the cost of slight loss to accuracy if needed.

The range of the stereo camera ADAS system

If you see the basic stereo equation (Figure 7) once again, then it is evident that to improve the maximum range of the system, the distance computation needs to be reasonably accurate for low disparities. That can be achieved by any of the following three methods. Each of these methods have associated trade offs for mechanical or electronic design and eventually system cost.

- (a) Use a smaller pixel size → If we use a smaller pixel size (let's say half), and if everything else stays the same, the range improves by about 50 percent (for the same accuracy)
- (b) Increase the distance between the two cameras → If "T" is increased to double, and

if everything else stays the same, the range improves by about 50 percent (for the same accuracy)

- (c) Change the focal length → If "f" is increased to double, and if everything else stays the same, the range improves by about 50 percent (for the same accuracy), but field of view narrows down
- (d) Use a computation system that calculates stereo disparity with sub-pixel accuracy

Although mathematically feasible, options (b) and (c) have a direct bearing on the physical attributes of the system. When a stereo system needs to be mounted in a car, typically it will have a fixed dimension or the requirement for the system to be as small as possible. This aesthetic need goes against increasing the distance between the cameras (T) or the focal length (f). Therefore, most practical options for an accurate stereo distance calculation system with high range and accuracy revolve around options (a) and (d) above.

The process

Figure 9 on the following page shows the high-level block diagram for data flow and compute chains to calculate the stereo disparity. Please note the absence of the camera calibration step that was present in the SFM block diagram in Figure 6, and that there is no need to search for features in the dense stereo disparity algorithm either. Identifying features and objects is required for SFM-based distance calculation methods that compute distance based on the size of an object.

The image rank transformation is most often the first or second step in the stereo image processing pipe. The purpose of this step is to ensure that

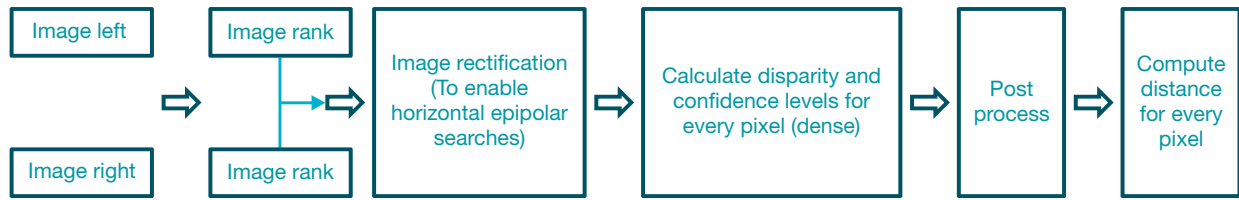


Figure 9: A high-level data and algorithm flow for stereo disparity-based distance computation.

the subsequent block comparisons between two images are robust to real-world noise conditions such as illumination or brightness changes between the left and right images [7]. These changes can be caused by many factors. Some of these include different illumination because of varied points of view from the two cameras and slight differences between the shutter speeds and other jitter artifacts that may cause the left and right images to be captured at slightly different points of time by the cameras.

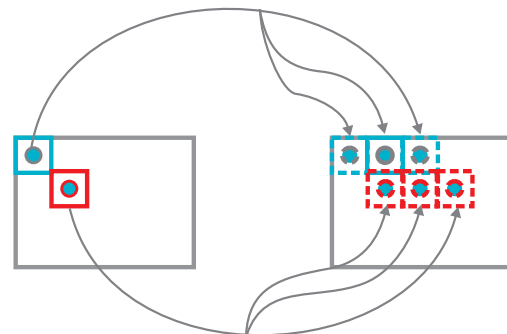
There are various papers and approaches suggested by researchers for different rank transform options for images and how they impact the robustness of disparity calculations [8]. The image rectification step in Figure 9 ensures that the subsequent disparity calculation can be performed along the horizontal epipolar search lines. The next steps in the process are actual calculation of disparity, confidence levels of the computation and post processing. The dense disparity calculation is mostly performed in spatial domain although there are some approaches suggested to calculate disparity in frequency domain [9].

These approaches attempt to take advantage of the fact that large FFTs can be calculated comparatively quickly, yet there are other complications involved in FFT that don't tilt the balance in its favor yet. Without the need to go deeper into that discussion in this article, it is a fair claim that most (if not all) productized stereo disparity algorithms are implemented in spatial domain. At the most basic

level, this analysis requires that for every pixel in the left (transformed) image, we need to pick a small block of pixels surrounding it.

Next, we need to search in the right side (transformed) image along the epipolar (horizontal) line until finding where the same block is located. This computation is performed for every possible value of disparity (from one to the maximum—64 or 128 or any other value). The difference (or cross correlation) between the left and right side block will approach minima (maxima) close to the actual value of disparity for the pixel. The performed “moving-window” block comparison and matching will calculate how much the block has moved, and the result will be used to calculate distance of that particular pixel in 3-D space. This process is shown in Figure 10. One such example of disparity calculation using rank transform followed by sum of absolute differences (SAD) based cost function minimization is given in [8].

**Shift block and compare in the right image for best match
Best match = disparity for pixel**



**Repeat calculation for every pixel in left image
For every possible value of disparity in right image**

Figure 10: Simple SAD-based block-comparison algorithm for finding disparity.

The SAD-based approach for finding disparity is elegant and sometimes too simplistic. The basic premise of this approach is that for a given block of pixels, the disparities are equal, however this is almost never true at the edges of the objects. If you review Figure 2 again and pay attention to the annotations made for forks of the motor cycle and the red box, you would quickly realize that there will be many adjacent pixels where disparity will be different. It is indeed normal since the “red box on the shelf” is about two meters farther from the camera than the “forks”. The disparity for a small block of pixels may change drastically at object boundaries and marginally for slanted or curved surfaces. The “cones and faces” image from Middlebury dataset ^[10] highlights this fact perfectly. The adjacent pixels found over one cone (slightly slanted surface) will have minor disparity changes, while the object boundaries will have large disparity differences. Using a simple SAD-based algorithm along with rank transform will leave large disparity holes on both occlusions such as the artifacts that are visible only in one camera and object boundaries.

To resolve such inaccuracies with deterministic run time, an elegant approach was suggested by ^[11].

This approach is called “semi global matching”. In this approach, a smoothness cost function is calculated for every pixel in more than one direction (4, 8 or 16). The cost function calculation is shown in Figure 12 below. The objective is to optimize the cost function $S(p,d)$ in multiple directions for every pixel and to ensure a smooth disparity map. The original paper for SGM suggested 16 directions for optimization of the cost function, though practical implementations have been attempted for 2, 4 and 8 directions as well.

$$L_r(p,d) = C(p,d) + \min \begin{cases} L_r(p-r,d) \\ L_r(p-r,d-1)+P1 \\ L_r(p-r,d+1)+P1 \\ \min_i L_r(p-r,i)+P2 \end{cases} - \min_k L_r(p-r,k)$$

$$S(p,d) = \sum_r L_r(p,d)$$

$r = 1$ to 16
 $L_r(p,d)$ = cost for pixel p at disparity d
 $C(p,d)$ = Matching cost function
 $P1$ = Penalty cost for a local disparity change of 1
 $P2$ = Penalty cost for a disparity change > 1
 $S(p,d)$ = Smoothness cost function after adding $L_r(p,d)$ in all 16 directions for disparity d

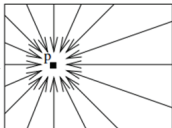


Figure 12: Optimization cost function equations for SGM.

A concrete implementation of SGM cost functions and optimization algorithm is shown in Figure 13 on the following page. With this pseudo-code segment, it is easy to assess the memory, computation and



Figure 11: Cones and faces from Middlebury dataset. The disparity calculation is performed using simple SAD. The disparity keeps changing marginally on the curved surfaces, while it changes drastically on the object boundaries. See the disparity holes in the fence on the top-right, other object discontinuities and occlusions on left border.

eventually hardware complexity requirements to enable SGM-based computation in real time.

```

Initialize C, disparity, S and Lr for every pixel
LOOP 1: For every pixel p
  LOOP 2: For every disparity d (1..k)
    Calculate C(p,dk) → SAD or Mutual Information (MI) based
    LOOP 3: For every direction r (1..16)
      Calculate Lr(p,d)
    END LOOP 3
    Calculate S(p,d) using equation in figure 12
    if S(p,dk) < Smin(p,dk) → disparity = dk, else disparity = dinit
  END LOOP 2
END LOOP 1
  
```

Figure 13: Pseudo code for implementation of SGM.

Computation and memory requirements for the disparity calculation

As you can well imagine, this calculation is compute heavy for ADAS applications. A typical front-facing stereo camera rig is a set of 1-Mpixel cameras operating at 30 frames per second. The first steps in the disparity calculation process are rank transforms. A typical rank transform is a census transform or a slightly modified version. The inputs required are both stereo images, while the outputs are census-transformed image pairs. The computation required for census transform for an $N \times N$ block around the pixel is to perform 60 million, $N \times N$ census transforms. Every census transform done for a pixel over a $N \times N$ block requires N^2 comparison operations. Some other

involved rank transforms need an N^2 point sort for every pixel. It is safe to assume that the minimum possible requirement is to run 60 million $\times N^2$ comparison operations for rank transformation in practical systems deployed on real vehicles for next few years.

The second step in the process requires image rectification to ensure that the epipolar disparity searches are needed on the horizontal lines. The third step is more interesting since it involves calculation of $C(p,d)$, $L_r(p,d)$ and $S(p,d)$ for every pixel and disparity combination (see Figure 13). If $C(p,d)$ is a block-wise SAD operation and the block size is $N \times N$, the required system range is ~200 meters and the accuracy of distance calculated required half-pixel disparity calculation then the system will require to calculate $C(p,d)$ for 64–128 disparity possibilities. The total compute requirements for $C(p,d)$ with these parameters are to perform 60 million $\times N^2 \times 128$ SAD operations every second.

The calculation of $L_r(p,d)$ needs to be done for every pixel in “r” possible directions, hence the calculation of this term (see Figure 13) needs to be done 60 million $\times 128 \times r$ times. The calculation for one pixel requires five additions (if you consider subtraction a special form of addition) and one minima-finding operation. Putting it together, the calculation of $L_r(p,d)$ per second needs 60 million $\times 128 \times r \times 5$ additions and 60 million $\times 128 \times r$ minima computations for four terms.

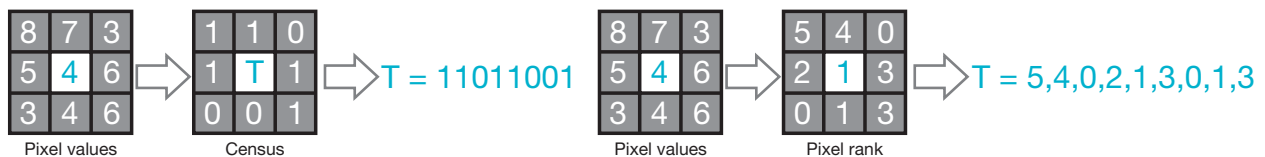


Figure 14: Rank transform examples for images. The left part of the image is simple census transform. The right half is called “complete rank transform” [7].

The calculation of $S(p,d)$ needs to be done r times for every possible pixel and disparity value, every computation of $S(p,d)$ requires “ r ” additions and one comparison. The total operations needed for calculating this per second are $60 \text{ million} \times 128 \times r$ additions and $60 \text{ million} \times 128$ comparisons.

Putting all three together, an accurate SGM-based disparity calculation engine, running on 1 Mpixel, 30-fps cameras and intending to calculate 128 disparity possibilities will need to perform approximately 1 Tera operations (additions, subtractions, minima finding) every second. To put this number in perspective, advanced general-purpose processors in embedded domain issue seven to ten instructions per cycle. Some of these instructions are SIMD type, i.e., they can tackle 8–16 pieces of data in parallel. Considering the best IPC that a general-purpose processor has to offer, a quad-core processor running at 2 GHz will offer about 320 Giga 64-bit operations. Even if we consider that most of the stereo pipeline will be 16 bits and the data can be packed in 64-bit bins with 100 percent efficiency, a quad-core general-purpose processor is hardly enough to meet the demands of a modern day ADAS stereo vision system. The objective of a general-purpose processor is to afford high-level programmability of all kinds. What it means is that designing a real-time ADAS stereo vision system requires specialized hardware.

Robustness of calculations

The purpose of ADAS vision systems is to avoid or at least minimize the severity of road accidents. More than 1.2 million people are killed every year due to road accidents, making it the leading cause

of death for people aged 15–29 years. Pedestrians are the most vulnerable road users, with more than 250,000 pedestrians succumbing to injuries each year. The major cause of road accidents is mistakes made by drivers either due to inattention or fatigue. Therefore, the most important purpose of an ADAS vision system for emergency braking is to reduce the severity and frequency of the accidents. That is a double-edged requirement since a vision system not only has to estimate the distances correctly with high robustness every video frame and every second, but also minimize the false positive scenarios. To ensure the ADAS system is specified and designed for the right level of robustness, ISO 26262 was created as an international standard for the specification, design and development of electronics system for automotive safety applications.

A little calculation here will bring out the estimated errors in computing distance for a stereo vision system. Please see Figure 15. If the error tolerances for the focal length (f) and the distance between the cameras (T) is 1 percent and the accuracy of disparity calculation algorithm is 5 percent, then the calculated distance (Z) will still be about 2.5 percent inaccurate. Improving the accuracy of the disparity calculation algorithm to a sub-pixel (quarter or half pixel) level therefore is important. This has two implications. The first being increased post-processing interpolation compute requirements of the algorithm and the hardware. The second requirement is more sophisticated and is related to ISO 26262.

$$Z = f T / d$$

If f , T & calculated d have a standard deviation of s_f , s_T & s_d respectively, then

$$s_Z = ((s_d)^2 + (s_T)^2 + (s_f)^2)^{1/2}$$

Figure 15: Statistical error estimation for calculated distance by a stereo vision system [13].

The architecture and design needs to ensure that both transient and permanent errors in the electronic components are detected and flagged within the fault tolerant time interval (FTTI) of the system. The calculation of FTTI and the other related metrics is beyond the scope of this article, yet it should suffice to point out that the electronic components used to build the system need to enable achieving the required ASIL levels for the ADAS vision system.

System hardware options and summary

In this article, we reviewed the effectiveness of various algorithm options in general and stereo-vision algorithms in particular to calculate distance for an automotive ADAS safety emergency braking system. Texas Instruments is driving deep innovation in the field of ADAS processing in general, and efficient and robust stereo-vision processing in particular.

There can be many different electronic system options to achieve the system design and performance objectives for an ADAS safety vision system. Heterogeneous chip architectures by Texas Instruments (TDA family) are suitable to meet the performance, power, size and ASIL functional safety targets for this particular application. A possible system block diagram for stereo and other ADAS systems using TI TDA2x and TDA3x devices and demonstrations of the technology are available at www.ti.com/ADAS.

References

- [1] Cave paintings: http://en.wikipedia.org/wiki/Cave_painting#Southeast_Asia
- [2] D. Scharstein, H. Hirschmüller, Y. Kitajima, G. Krathwohl, N. Nesić, X. Wang, and P. Westling. “High-resolution stereo datasets with subpixel-accurate ground truth”. In *German Conference on Pattern Recognition (GCPR 2014)*, Münster, Germany, September 2014
- [3] Figure credit: “Vision-based Object Detection and Tracking”, HyunggiC!, http://users.ece.cmu.edu/~hyunggiC/vision_detection_tracking.html
- [4] Image credit: pixabay.com
- [5] 3D Structure from 2D Motion, <http://www.cs.columbia.edu/~jebara/papers/sfm.pdf>
- [6] Chapter 7 “Stereopsis” of the textbook of E. Trucco and A. Verri, *Introductory Techniques for 3-D Computer Vision*, Prentice Hall, NJ, 1998 and lecture notes from <https://www.cs.auckland.ac.nz/courses/compsci773s1t/lectures/773-GG/topCS773.htm>
- [7] “The Complete Rank Transform: A Tool for Accurate and Morphologically Invariant Matching of Structures”, Mathematical Image Analysis Group, Saarland University, <http://www.mia.uni-saarland.de/Publications/demetz-bmvc13.pdf>
- [8] “A Novel Stereo Matching Method based on Rank Transformation”, Wenming Zhang, Kai Hao*, Qiang Zhang, Haibin Li Reference: <http://ijcsi.org/papers/IJCSI-10-2-1-39-44.pdf>
- [9] “FFT-based stereo disparity estimation for stereo image coding”, Ahlvers, Zoelzer and Rechmeier

- [10] “Semi-Global Matching”, <http://lunokhod.org/?p=1356>
- [11] “Accurate and Efficient Stereo Processing by Semi-Global Matching and Mutual Information”, <https://ieeexplore.ieee.org/document/1467526>
- [12] “More than 270,000 pedestrians killed on roads each year”, http://www.who.int/mediacentre/news/notes/2013/make_walking_safe_20130502/en/
- [13] “Propagation of Error”, http://chemwiki.ucdavis.edu/Analytical_Chemistry/Quantifying_Nature/Significant_Digits/
- [14] Optical flow reference: “Structure from Motion and 3D reconstruction on the easy in OpenCV 2.3+ [w/ code]” <http://www.morehanttechnical.com/2012/02/07/structure-from-motion-and-3d-reconstruction-on-the-easy-in-opencv-2-3-w-code/>
- [15] Mutual information reference: “Mutual Information as a Stereo Correspondence Measure”, http://repository.upenn.edu/cgi/viewcontent.cgi?article=1115&context=cis_reports
- [16] Image entropy analysis using Matlab[®]
- [17] Image credit: “Engines idling in New York despite law”, CNN News, <http://www.cnn.com/2012/02/06/health/engines-new-york-law/>

Important Notice: The products and services of Texas Instruments Incorporated and its subsidiaries described herein are sold subject to TI's standard terms and conditions of sale. Customers are advised to obtain the most current and complete information about TI products and services before placing orders. TI assumes no liability for applications assistance, customer's applications or product designs, software performance, or infringement of patents. The publication of information regarding any other company's products or services does not constitute TI's approval, warranty or endorsement thereof.

The platform bar is a trademark of Texas Instruments. All other trademarks are the property of their respective owners.

IMPORTANT NOTICE AND DISCLAIMER

TI PROVIDES TECHNICAL AND RELIABILITY DATA (INCLUDING DATASHEETS), DESIGN RESOURCES (INCLUDING REFERENCE DESIGNS), APPLICATION OR OTHER DESIGN ADVICE, WEB TOOLS, SAFETY INFORMATION, AND OTHER RESOURCES "AS IS" AND WITH ALL FAULTS, AND DISCLAIMS ALL WARRANTIES, EXPRESS AND IMPLIED, INCLUDING WITHOUT LIMITATION ANY IMPLIED WARRANTIES OF MERCHANTABILITY, FITNESS FOR A PARTICULAR PURPOSE OR NON-INFRINGEMENT OF THIRD PARTY INTELLECTUAL PROPERTY RIGHTS.

These resources are intended for skilled developers designing with TI products. You are solely responsible for (1) selecting the appropriate TI products for your application, (2) designing, validating and testing your application, and (3) ensuring your application meets applicable standards, and any other safety, security, or other requirements. These resources are subject to change without notice. TI grants you permission to use these resources only for development of an application that uses the TI products described in the resource. Other reproduction and display of these resources is prohibited. No license is granted to any other TI intellectual property right or to any third party intellectual property right. TI disclaims responsibility for, and you will fully indemnify TI and its representatives against, any claims, damages, costs, losses, and liabilities arising out of your use of these resources.

TI's products are provided subject to TI's Terms of Sale (www.ti.com/legal/termsofsale.html) or other applicable terms available either on ti.com or provided in conjunction with such TI products. TI's provision of these resources does not expand or otherwise alter TI's applicable warranties or warranty disclaimers for TI products.

Mailing Address: Texas Instruments, Post Office Box 655303, Dallas, Texas 75265
Copyright © 2020, Texas Instruments Incorporated